Optical loss study of molecular layer for a cryogenic interferometric gravitational-wave detector

Satoshi Tanioka,[1,2,*] Kunihiko Hasegawa,[3] and Yoichi Aso[1,2,†]

[1]*The Graduate University for Advanced Studies (SOKENDAI), Mitaka, Tokyo 181-8588, Japan*
[2]*National Astronomical Observatory of Japan, Mitaka, Tokyo 181-8588, Japan*
[3]*Institute for Cosmic Ray Research, The University of Tokyo, Kashiwa, Chiba 277-8582, Japan*

(Received 25 June 2020; accepted 14 July 2020; published 27 July 2020)

The detection of gravitational waves provides us with a deep insight into the Universe. In order to increase the number of detectable gravitational-wave sources, several future gravitational-wave detectors will operate with cryogenic mirrors. Recent studies, however, showed that residual gas molecules inside the vacuum chamber adhere to the cryogenic mirror surface and form a molecular layer which grows with time. This growing molecular layer introduces an additional optical loss in the mirror which can decrease the detector's performance. We theoretically estimate the optical loss by the molecular layer in a cryogenically operated gravitational-wave detector. The impact on a cryogenic gravitational-wave detector is discussed based on the results of the optical loss estimation.

DOI: 10.1103/PhysRevD.102.022009

I. INTRODUCTION

The first detection of gravitational waves (GWs) from a binary black hole (BBH) by Advanced LIGO (aLIGO) opened a new window to search the Universe [1]. In the following observation run, aLIGO and Advanced Virgo detected a GW from a binary neutron star merger which enabled us to observe a counterpart by electromagnetic observations [2,3]. Improved sensitivity is indispensable to detecting further GW events and investigating the nature of GWs, the origin of the source, and other astrophysical properties [4]. The sensitivity of the current ground-based interferometric gravitational-wave detectors (GWDs) is mainly limited by the quantum noise and thermal noise [5]. For the case of aLIGO, which operates at room temperature with fused silica test mass mirrors, the coating thermal noise limits the most sensitive frequency range around 100 Hz, which is an important frequency band to detect GWs from compact binary coalescences. Therefore, the reduction of thermal noise using cryogenic mirrors is a promising approach to achieving a larger number of detections and observing a wider variety of sources [6].

The Einstein Telescope (ET), a third-generation GWD in Europe, and LIGO Voyager, a substantial upgrade of aLIGO, are planning to employ cryogenic silicon mirrors whose temperatures are 10 K and 123 K, respectively [7–9]. Fused silica, the material used in the current room-temperature GWDs, has a large mechanical loss at cryogenic temperature, which leads to large thermal noise and is not suitable for a cryogenic GWD [10]. Silicon has a small mechanical loss and consequently a low Brownian noise under cryogenic temperature [11]. In addition, silicon has the unique advantage that its substrate thermoelastic noise vanishes at 18 K and at 123 K, where its coefficient of thermal expansion crosses zero [12]. However, as silicon is opaque for wavelengths shorter than 1100 nm and has small absorption only for wavelengths longer than 1400 nm, the wavelength of the main laser should be within the range of 1400 to 2100 nm [13]. Therefore, the wavelength of the main laser is chosen to be 1550 and 2000 nm for ET and for LIGO Voyager, respectively [8,9].

KAGRA, a gravitational-wave detector constructed in Japan, is operated with cryogenically cooled sapphire mirrors, aiming to reduce the thermal noises and to improve the sensitivity [14,15]. The cryogenic mirrors in KAGRA, however, suffer from molecular layer formation on the mirror surfaces [16]. This is caused by continuous molecular transportation from the room-temperature beam duct where water molecules can easily detached from the surface. When gas molecules hit a cryogenic mirror surface, they lose their kinetic energy and adhere onto the surface, which is the so-called cryopumping effect. Therefore, the collisions of gas molecules create a molecular layer on top of the cryogenic mirror surface. We call such a molecular layer a cryogenic molecular layer (CML) in this paper. The properties of the mirror, i.e., the reflectance and transmittance, change due to the growth of the CML. The change in mirror properties can increase the noise level related to the beam power [17]. Moreover, the thermal noise induced by the CML can become a limiting noise source in the ET [18]. Thus, the sensitivity of

*satoshi.tanioka@grad.nao.ac.jp
†yoichi.aso@nao.ac.jp

cryogenic GWDs can be deteriorated by the CML formation. The impact of the CML on optical loss has been experimentally estimated on a small-scale cryogenic system [19] and studied for the case of KAGRA [17]. The coating thermal noise (CTN) from the CML has also been studied for the case of the ET [18], though the impact on optical loss was not discussed there.

In this article, first, we derive a theoretical model of the optical loss induced by the CML in a cryogenic GWD. Then we show how the optical loss of a CML affects a cryogenic interferometric GWD. Finally, we discuss the impacts of the CML on cryogenic GWDs and possible solutions to relieve it.

II. OPTICAL LOSS

Low-optical-loss mirrors are vital for precision laser interferometry [20,21]. As shown in Fig. 1, optical loss in the mirror is introduced mainly by two paths—optical scattering and absorption. The test mass mirrors used in GWDs are manufactured with state-of-the-art technologies to meet the requirements on optical losses [22]. A molecular layer, however, generates additional optical loss, which can hinder us from operating the detector at a cryogenic temperature and achieving the design sensitivity. Especially, the optical absorption generates an additional heat load to a cryogenic mirror, and its temperature can be increased by this effect. In this section, we review the derivation of the optical loss by a CML on a test mass mirror. For more details, one can see Ref. [23].

A. Scattering

A beam reflected by a mirror is scattered by the imperfections of the mirror surface, which causes an optical loss and decreases the arm cavity power in GWDs. Moreover, the scattered light can become a technical noise source in GWDs by recombining with the main beam [24,25]. Therefore, the scattering by the CML can reduce the sensitivity of GWDs. In this section, we theoretically derive the amount of optical loss induced by scattering in the CML.

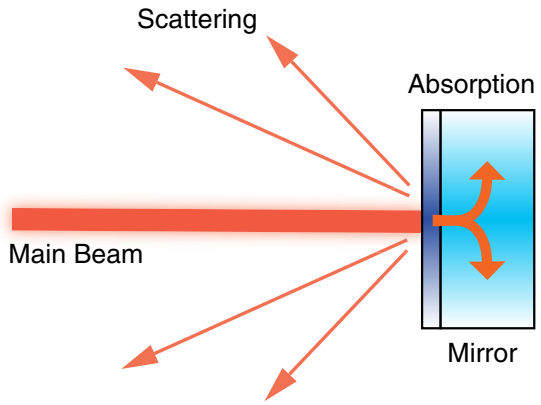

FIG. 1. Schematic drawing of the optical loss in the test mass mirror. The scattering and absorption lead to less arm cavity power, which decreases the sensitivity of GWDs. Furthermore, the optical absorption introduces an additional heat load to a cryogenic mirror.

The ratio between the total reflected beam power and that of scattered light, called total integrated scattering (TIS), is defined as [26]

$$\mathrm{TIS} \sim \frac{P_{\mathrm{sca}}}{P_0 R}, \tag{1}$$

where P_0 is the incident beam power, P_{sca} is the power of the scattered light, and R is the reflectance of the CML surface. For the case of the angle of incidence equaling zero, such as in the arm cavities in GWDs, the TIS can be calculated as [27]

$$\mathrm{TIS} = 1 - \exp\left\{-\left(\frac{4\pi\sigma}{\lambda}\right)^2\right\}, \tag{2}$$

where

$$\sigma^2 = 2\pi \int_0^{\frac{1}{\lambda}} \mathrm{PSD}(f) f \mathrm{d}f. \tag{3}$$

Here λ is the laser wavelength. $\mathrm{PSD}(f)$ $[\mathrm{m}^4]$ represents the 2D surface power spectral density, and f $[1/\mathrm{m}]$ is the spatial frequency.

Assuming uniform molecular adsorption on a cryogenic mirror surface, the incident molecular flux to the unit area follows the Poisson distribution. Therefore, the standard deviation of the number of molecules is given by $\sqrt{\langle N \rangle}$, where N is the average number of molecules. The relationship between the thickness of the CML, t, and N can be expressed as

$$t = N\left(\frac{M}{\rho N_A}\right)^{1/3}, \tag{4}$$

where ρ $[\mathrm{kg/m^3}]$ represents the density of the CML, N_A $[1/\mathrm{mol}]$ is the Avogadro number, and M $[\mathrm{kg/mol}]$ is the molecular mass. From Eq. (4), the relation between the mean thickness of the CML, $\langle t \rangle$, and its standard deviation, $\sigma_{\langle t \rangle}$, can be written as

$$\sigma_{\langle t \rangle} = \left(\frac{M}{\rho N_A}\right)^{1/3} \sqrt{\langle N \rangle} = \left(\frac{M}{\rho N_{\mathrm{A}}}\right)^{1/6} \sqrt{\langle t \rangle}. \tag{5}$$

PSD, which follows this distribution, can be calculated as [28]

$$\mathrm{PSD}(f) = \pi \sigma_{\langle t \rangle}^2 \xi^2 \exp[-(\pi f \xi)^2], \tag{6}$$

where ξ is the correlation length which characterizes the periodic length of the roughness along the surface. Thus, the scattered power by the CML can be expressed as

$$P_{\mathrm{sca}} \sim P_0 R\left[1-\exp\left\{-\frac{32\pi^4\sigma_{\langle t\rangle}^2\xi^2}{\lambda^2}\int_0^{\frac{1}{\lambda}} e^{-(\pi f\xi)^2} f\mathrm{d}f\right\}\right]. \quad (7)$$

Assuming the surface roughness of the CML, Eq. (7) allows us to estimate the optical loss generated by the scattering.

B. Optical absorption

Another factor leading to an optical loss is optical absorption. In particular, the optical absorption in a cryogenic mirror plays a crucial role in selecting the parameters of GWD because of an additional heat load on the test mass mirror. For the case of a GWD, a Fabry-Pérot cavity is embedded in the arm to improve the sensitivity [7,9,15]. Hence, the laser power inside the arm cavity becomes extraordinarily large, and the optical absorption introduced by the CML can become a critical heat source in the cryogenic test mass. Absorption in the AR surface can be negligible because of a much lower laser power on the surface than on the HR side.

In the same manner as the previous work [17], assuming that the amplitude of the laser intensity inside a medium follows the Lambert-Beer law, the total amount of absorption by the CML, A_{CML}, with the thickness of d_{CML} is expressed as

$$A_{\mathrm{CML}} = P_{\mathrm{CML}}[1-\exp(-\alpha_{\mathrm{CML}} d_{\mathrm{CML}})], \quad (8)$$

where P_{CML} is the laser power incoming to the CML and $\alpha_{\mathrm{CML}} = 4\pi\mathrm{Im}(N_{\mathrm{CML}})/\lambda$ is the absorption coefficient of the CML. Assuming that the Lambert-Beer law holds for the CML, the amount of optical absorption by the CML can be estimated as

$$A_{\mathrm{CML}} = \frac{1-R_{\mathrm{CML}}}{\pi}\mathcal{F}_{\mathrm{arm}} G P_{\mathrm{in}}[1-\exp(-2\alpha_{\mathrm{CML}} d_{\mathrm{CML}})], \quad (9)$$

where R_{CML} is the power reflectance of the CML, $\mathcal{F}_{\mathrm{arm}}$ is the finesse of the arm cavity, and G is the power recycling gain. It should be noted that these values are dependent on the thickness of the CML. The index of the exponential is doubled because the beam goes through the CML twice.

III. IMPLICATIONS TO EXPERIMENT

Some future GWDs plan to use cryogenic mirrors to achieve better sensitivity. Low optical absorption is critical for cryogenic GWDs, both to maintain the cryogenic temperature of the test mass and to achieve the design sensitivity. As the arm cavity power is designed to be 18 kW and 3 MW for ET and LIGO Voyager, respectively, additional heat absorption introduced by the CML can become a critical problem in maintaining the cryogenic temperature of the test masses. We show the impacts of CMLs on the future GWDs which adopt cryogenic mirrors.

In order to evaluate the impact of the CML, we need to make several assumptions. First, we assume that the CML is composed of water as the previous works did [17,18]. In addition, the water molecular layer is formed as amorphous ice [29]. The refractive index of amorphous ice at cryogenic temperatures has been studied for wavelengths of 210–757 nm [30]. We derive the refractive index at 1064, 1550, and 2000 nm by extrapolation using the Lorentz-Lorenz equation, which gives the relation between the density ρ and the refractive index $n(\lambda)$ as

$$R(\lambda) = \frac{1}{\rho}\frac{n(\lambda)^2-1}{n(\lambda)^2+2}, \quad (10)$$

where $R(\lambda)$ is the specific refraction, which can be expressed as

$$R(\lambda) = \sqrt{\frac{D_1\lambda^2}{\lambda^2-C_1}+\frac{D_2\lambda^2}{\lambda^2-C_2}}. \quad (11)$$

C_1, C_2, D_1 and D_2 are the parameters to explain the experimental result, and C_1 and C_2 are given by the previous report [30]. D_1 and D_2 are obtained by fitting the data shown in Ref. [30] using Eq. (10). The results are shown in Fig. 2, and the values of parameters are listed in Table I. As there is no characteristic structure of the H_2O molecule within the wavelength we discuss here, its refractive index monotonically decreases gently until 2 μm, as shown in Ref. [31]. Therefore, this extrapolation is a reasonable assumption to evaluate the effect of the CML. Furthermore, we use the literature value for the estimation of optical absorption. The absorption coefficient of amorphous ice has been reported at the temperatures of 40 K and 140 K [32]. As the temperature dependence of the absorption coefficient is so weak between 40 K and 140 K, we adopt these literature values to calculate the absorption

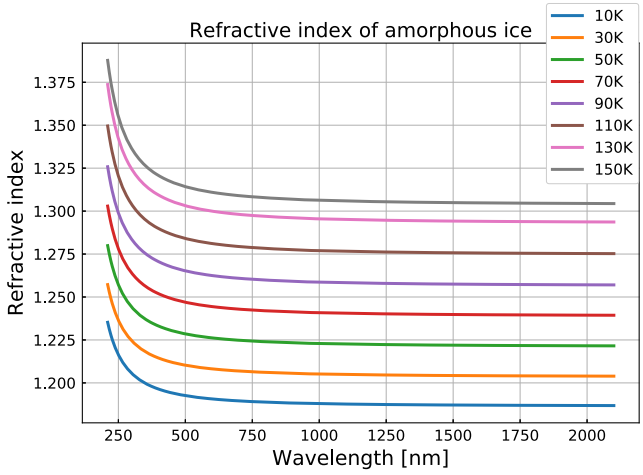

FIG. 2. Refractive index of the amorphous ice for various temperatures derived by the Lorentz-Lorenz equation.

TABLE I. The parameters to calculate the refractive indices. C_1 and C_2 are given by the previous report [30]. D_1 and D_2 are obtained by fitting using Eq. (10).

Symbol	$\sqrt{C_1}$	$\sqrt{C_2}$	D_1	D_2
Value	71	134	0.00996	0.0319

at 123 K. In addition, we assume that the absorption coefficient at 10 K is almost the same as the value at 40 K. The parameters which are used for the estimation are shown in Table II.

A. KAGRA

KAGRA is operated with cryogenically cooled sapphire mirrors at the temperature of 22 K with a laser source of wavelength 1064 nm [14,15]. The cryogenic mirrors in KAGRA are reported to suffer from the CML formation on the surfaces [16]. Previous study reported the amount of absorbed heat power in KAGRA, though the impact of scattering was not taken into account [17]. Here, we show the optical loss in KAGRA including scattering and revisit the heat absorption for comparison with other cryogenic GWDs. For the case of KAGRA, test masses are cooled by heat conduction using sapphire fibers. The estimated heat extraction capacity is about 0.72W [34].

Figure 3 shows the estimated optical loss by scattering and absorption for KAGRA. Optical loss induced by scattering is less than 1 ppm as long as the thickness of the CML is below 1 μm, even if the correlation length ξ is equal to $\sigma_{\langle t\rangle}$. Assuming a uniform molecular injection onto the mirror surface, the correlation length, ξ, becomes small because it forms a tidy and smooth surface. Therefore, the impact of scattering can be negligible when the thickness of the CML is below 1 μm.

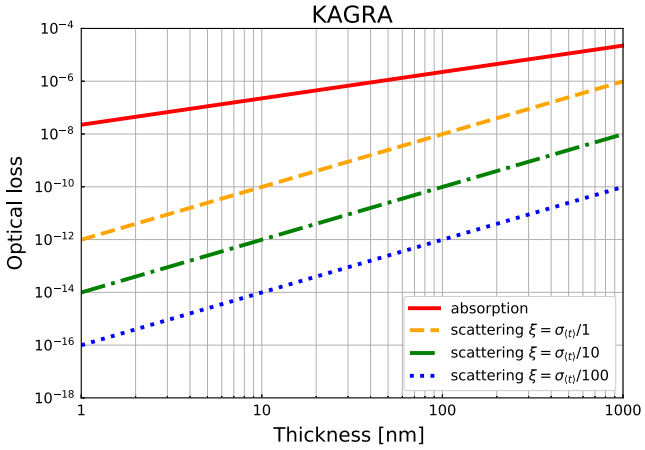

FIG. 3. Scattering and absorption losses induced by the CML for the case of KAGRA. The assumed wavelength is $\lambda = 1064$ nm. The red solid line represents the absorption, while the yellow dashed line, green dash-dotted line, and blue dotted line represent the scattering with the correlation lengths of $\xi = \sigma_{\langle t\rangle}, \sigma_{\langle t\rangle}/10$ and $\sigma_{\langle t\rangle}/100$, respectively.

On the other hand, the absorption is relatively large and has the potential to prevent cryogenic operation due to the additional heat load to the test masses. For the case of KAGRA, as the intracavity power becomes about 370 kW, absorption at the ppm level exceeds the capacity of heat extraction and leads to an increase in the test mass temperature. In other words, a CML with a few tens of nm thickness can increase the temperature of the test mass. Here we focus on a thin thickness range to estimate the heat absorption in which the power reflectance of the CML, the finesse of the arm cavity, and the power recycling gain can be considered to be constant. Therefore, the absorbed power by the CML is proportional to the thickness of the CML: $A_{\mathrm{CML}} \propto \alpha_{\mathrm{CML}} d_{\mathrm{CML}}$.

TABLE II. The assumed parameters of cryogenic GWDs [8,9,33]. Here we assume that the CML is composed by amorphous ice. The refractive indices of amorphous ice are derived by the fitting using the Lorentz-Lorenz equation. It should be noted that the refractive indices at 22 K and 123 K are the averaged values of those at 10 K and 30 K, and those at 110 K and 130 K, respectively. The absorption coefficient of the CML is assumed to be the literature value [31,32].

Parameters	Symbol	KAGRA	ET	Voyager
Temperature of the test mass	T	22 K	10 K	123 K
ITM transmittance	T_{ITM}	0.4%	0.7%	0.2%
ETM transmittance	T_{ETM}	7 ppm	6 ppm	5 ppm
PRM transmittance	T_{PRM}	10%	4.6%	4.92%
Loss inside the arm cavity	$T_{\mathrm{loss,arm}}$	93 ppm	75 ppm	10 ppm
Laser wavelength	λ	1064 nm	1550 nm	2000 nm
Laser power	P_{in}	67 W	3 W	152 W
Mirror thickness	d_{mir}	15 cm	50 cm	55 cm
Refractive index of amorphous ice	n	1.20	1.19	1.28
Absorption coefficient of amorphous ice	α_{CML}	2.2×10 1/m	2.0×10^3 1/m	8.0×10^3 1/m
Absorption in test mass	α_{mir}	50 ppm/cm	3.2×10^{-2} ppm/cm	10 ppm/cm
Extractable heat	Q	0.72 W	100 mW	10 W

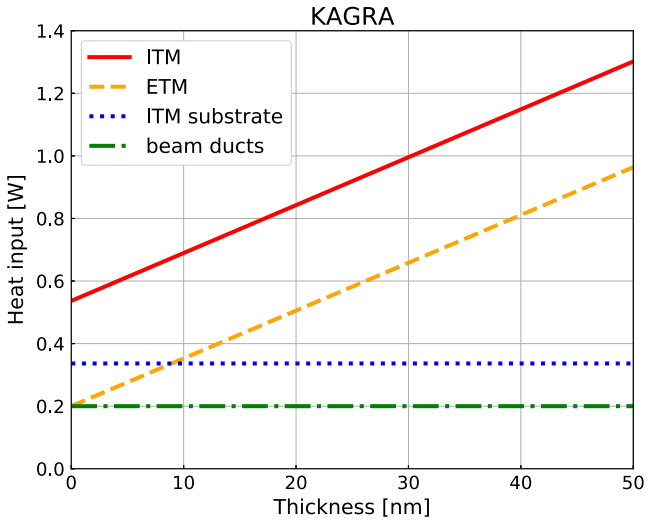

FIG. 4. Heat input to each test mass mirror in KAGRA induced by the optical absorption of the CML. Due to the absorption of sapphire substrate, the heat input to the ITM is larger than that of the ETM. As a result of the absorption of amorphous ice, the heat load to the ITM exceeds 1 W when the thickness becomes larger than about 30 nm. It should be noted that the radiation from beam ducts is taken into account for the case of KAGRA.

Figure 4 shows the heat absorption of the input test mass (ITM) and end test mass (ETM) of KAGRA. In this calculation, the absorption in the substrate and radiation from the beam ducts are taken into account. Once the thickness becomes larger than about 10 nm, the heat input to the ITM exceeds the tolerable value, 0.72 W, and the temperature of the test mass cannot reach the target value. Therefore, the thickness of the CML should be kept less than about 10 nm in order to maintain the temperature of the test mass. For the ETM, the heat input is smaller as long as the thickness of the CML is smaller than about 30 nm.

B. Einstein Telescope

The Einstein Telescope is a planned European GWD which will use cryogenic silicon mirrors at the temperature of 10 K with a laser source of wavelength 1550 nm for the low-frequency part [7]. Extracting the heat generated by the absorption at the mirror surfaces has to be done by the thermal conduction of the suspension fibers because of the significantly low thermal radiation at the cryogenic temperature of 10 K. The capacity of heat extraction by the suspension fibers is only 100 mW [8]. Therefore, the optical absorption should be kept as small as possible.

Figure 5 shows the result of the optical loss by the scattering and absorption for the ET. The impact of scattering can be negligible when the thickness of the CML is below 1 μm in the same manner as with KAGRA. On the other hand, the absorption is remarkably large because of the use of a longer-wavelength laser and has the potential to prevent a cryogenic operation due to the additional heat load to the test mass.

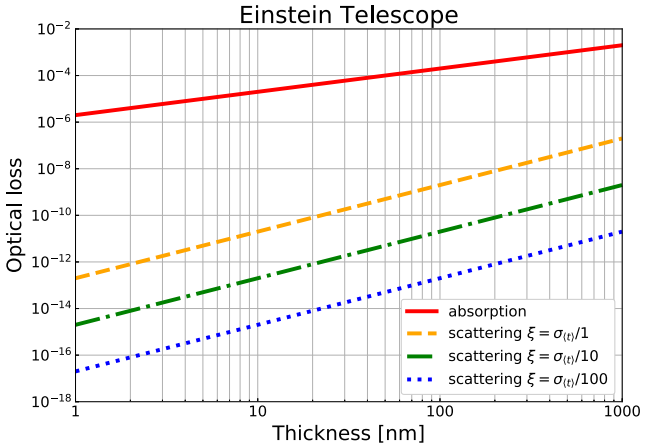

FIG. 5. Scattering and absorption loss for the case of the ET. The assumed wavelength is $\lambda = 1550$ nm. The red solid line represents the absorption, while the yellow dashed line, green dash-dotted line, and blue dotted line represent the scattering with the correlation lengths of $\xi = \sigma_{\langle t \rangle}, \sigma_{\langle t \rangle}/10$ and $\sigma_{\langle t \rangle}/100$, respectively.

Figure 6 shows the heat absorption of the ITM and ETM of the ET. Once the thickness becomes larger than a few nm, the heat input to the test masses exceeds the tolerable value, 100 mW, and the temperature of the test mass cannot reach the target value. Therefore, the thickness of the CML should be kept to less than 1 nm in order to maintain the temperature of the test masses.

C. LIGO Voyager

LIGO Voyager is a substantial upgrade of aLIGO, aiming to improve the inspiral range by a factor of 4 to 5 [9].

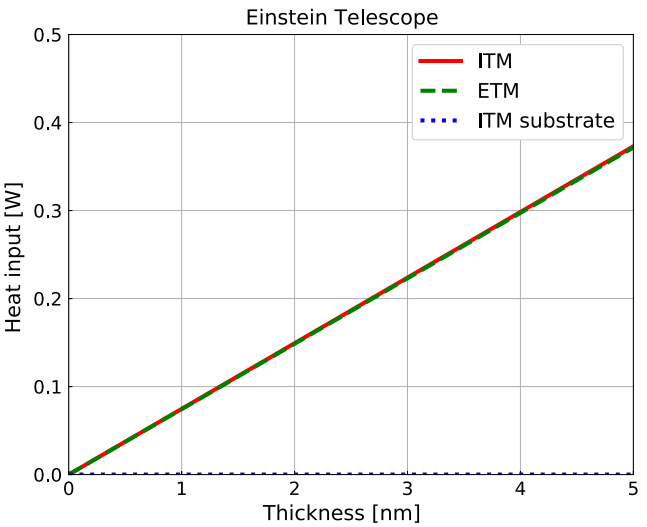

FIG. 6. Heat input to each test mass mirror in the ET induced by the optical absorption of the CML. As a result of strong absorption of amorphous ice, the heat load to the test mass exceeds 100 mW even when the CML thickness is only a few nm. It should be noted that the radiation from the beam ducts is not taken into account for the case of the ET.

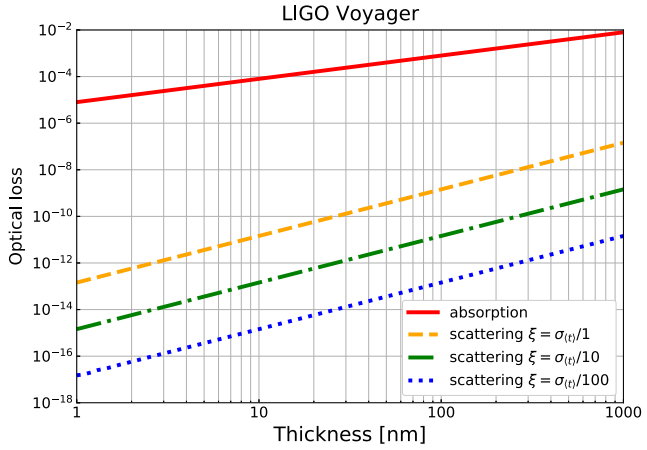

FIG. 7. Scattering and absorption loss for the case of LIGO Voyager. The assumed wavelength is $\lambda = 2000$ nm. In the same manner as the case of the ET, the red solid line represents the absorption, while the yellow dashed line, green dash-dotted line, and blue dotted line represent the scattering with the correlation lengths of $\xi = \sigma_{\langle t \rangle}, \sigma_{\langle t \rangle}/10$ and $\sigma_{\langle t \rangle}/100$, respectively.

Silicon is also a candidate material for LIGO Voyager test masses and will be cooled down to 123 K. The laser wavelength is chosen to be 2 μm for LIGO Voyager in order to take advantage of the lower absorption of amorphous silicon coating. The absorption coefficient of water molecules is, however, larger than that at the wavelength of 1.5 μm. Furthermore, the arm cavity power is much larger than the case of ET, 3 MW. Therefore, the heat absorption when the CML is formed on the silicon mirror can become a serious heat source, which prevents operation at the cryogenic temperature of 123 K.

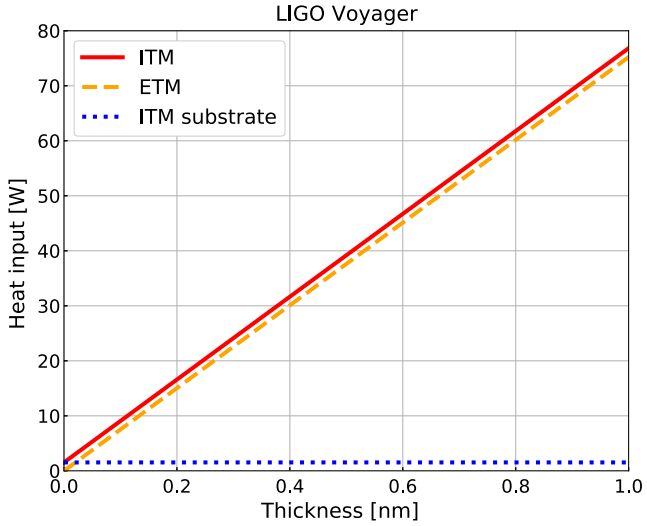

FIG. 8. Heat input to each test mass mirror in LIGO Voyager induced by the optical absorption of the CML. It should be noted that the radiation from the beam ducts is not taken into account for the case of LIGO Voyager.

Figure 7 shows the estimated optical loss by scattering and absorption for LIGO Voyager. Assuming uniform molecular injection onto the mirror surface, the impact of scattering can be negligible as long as the thickness of the CML is below 1 μm, in the same manner as the cases of KAGRA and the ET. On the other hand, the loss due to absorption is much larger than the scattering and can be harmful for cryogenic operation.

Figure 8 shows the heat absorption of the ITM and ETM of LIGO Voyager. The heat load generated by the optical absorption is extremely large, as the injected laser power is much larger than that of the ET. Even if the thickness is less than 1 nm, the heat load is still more than 10 W for both the ITM and ETM cases. This indicates that the test mass cannot be cooled down to 123 K. Thus, the heat absorption due to the CML may become a critical problem for LIGO Voyager.

IV. DISCUSSION

The optical absorption generated by the CML can be critical for cryogenic GWDs because of the unwanted heat load. Once the heat load exceeds the cooling capacity, the temperatures of test masses will increase. Eventually, the test mass reaches a thermal equilibrium state at some point. For the case of LIGO Voyager, the test mass temperature may become about 150 K, because the desorption of molecules starts around 150 K [23].

The growth rate of the CML is an important factor for operating a cryogenic GWD at the target test mass temperature. The growth rate measured in KAGRA is $\eta = (27 \pm 2)$ nm/day [17]. This growth rate can be reduced by a factor of 50 for the case of KAGRA by achieving the design vacuum level. Nevertheless, the growth rate is still about 0.5 nm/day, and a CML of a few nm thickness can be formed within several days. Therefore, a system to reduce the formation of a CML is indispensable.

Several passive ways to avoid the CML formation have been proposed. For example, a bake-out system for the arm cavity pipe is planed to be installed in the ET [8]. This system can remove the residual molecules in the pipe and exhaust by vacuum pumps before cooling down. Therefore, the CML formation on the cryogenic mirror in the ET should be significantly reduced. Using a longer cryogenic duct is another way to avoid the CML formation [17]. Operating at a high vacuum level is also essential for the cryogenic GWDs.

An active approach to remove the CML is also important. By heating up the test mass to about 200 K, the CML can be removed. This method, however, involves recooling of the test mass, which leads to a dead time of observation. It takes an order of one month to cool down the whole system for the case of KAGRA [33]. Therefore, cryogenic operation—in other words, operation with the best sensitivity—and duty cycle are in a relationship of trade-off if we adopt this method to remove the CML. One possible

way to solve this problem is to illuminate the cryogenic mirror with a CO_2 laser in the same manner as the thermal compensation system implemented in aLIGO [35]. By illuminating a CO_2 laser, the adsorbed molecules obtain kinetic energies and can desorb from the mirror surface. This laser desorption system only heats up the test mass, and the recooling period should be significantly improved. Combined with the passive reduction method, the observation time with better sensitivity can be enhanced.

It should also be noted that we can estimate the amount of CML in the arm cavity indirectly by measuring the finesse, as the finesse is related to the optical loss. The finesse of the arm cavity can be estimated by the ringdown measurement [36]. We can obtain the decay time of the transmitted light power, τ, by a measurement which relates the finesse as

$$\mathcal{F} = 2\pi f_{\mathrm{FSR}}\tau, \tag{12}$$

where f_{FSR} is the free spectral range of the cavity. From the obtained finesse value, we can estimate the total amount of CML in the arm cavity, and it can be a guide to decide the timing to illuminate the desorption laser if it is implemented. The thickness on each mirror, however, cannot be predicted individually by this method.

In this study, we estimate the optical loss from already formed CMLs. However, in the case of ET and Voyager, the formation of CML may be prevented in the first place, because of the high absorption of the amorphous H_2O ice at 1.5 and 2 μm. If the water molecules receive enough energy from the illuminated laser, they may desorb before forming a thick enough CML to cause trouble. In order to understand this process, we need to analyze the interaction between the laser photons and a water molecule while it is trapped in a cold amorphous ice. In addition, we assume that the Lambert-Beer law can be used to estimate the optical absorption by the CML. A previous research reported that this law holds for a silver layer much thinner than the wavelength [37]. However, validation of the Lambert-Beer law for the case of a CML is a subject of further study. Such studies are essential to fully understanding the impact of CMLs on the future cryogenic GWDs.

V. CONCLUSION

Cryogenic operation of a GWD is a promising way to improve the sensitivity of the detector by reducing the thermal noise. A cryogenic mirror, however, has a technical problem caused by adsorption of residual gas molecules. We presented the impact of the optical loss introduced by the CML formed on a cryogenic mirror. The effect of scattering loss can be negligible as long as the thickness of the CML is below 1 μm. On the other hand, the optical absorption becomes a critical problem for cryogenic operation because of an additional heat load to the cryogenic system. For the case of KAGRA, when the thickness of CML becomes larger than about 10 nm, the heat input can exceed the tolerable value. Furthermore, even when the thickness of CML is about 1 nm, the absorbed heat exceeds the capacity for both the ET and LIGO Voyager. Therefore, the CML on a cryogenic mirror can hinder us from operating the detector at the designed cryogenic temperature and can reduce the number of detectable GWs.

In order to mitigate the impact of the CML, a sophisticated cryogenic system is necessary. One possible approach is to implement an active desorption system in which a CO_2 laser is used. Passive approaches to reduce the formation rate are to develop a bake-out system, which is planned in the ET, or to use longer cryogenic ducts. In order to achieve the desirable sensitivity and stable operation of cryogenic GWDs, further studies are needed for both active and passive ways to solve the problems of CMLs.

ACKNOWLEDGMENTS

This work was supported by JSPS KAKENHI Grant No. JP18K03681 and JSPS Grant-in-Aid for Specially Promoted Research No. 26000005. This work was partially supported by Research Fund for Students of the Department of Astronomical Science, The Graduate University for Advanced Studies, SOKENDAI. This paper carries JGW Document No. JGW-P2011765.

APPENDIX: DERIVATION OF OPTICAL ABSORPTION

We derive Eq. (8) in this section. The laser power density inside a medium $I(z)$ follows the Lambert-Beer law as

$$I(z) = I_{\mathrm{s}}\exp(-\alpha z), \tag{A1}$$

where z represents the depth of a medium from its surface, I_{s} is the laser power density at the surface, $z = 0$, and α is the absorption coefficient. Assuming a Gaussian beam with a beam radius of w_0, the profile of the laser power intensity can be written as

$$\begin{aligned} I_r &= I_0\exp\left(-\frac{2r^2}{w_0^2}\right) \\ &= \frac{2P_0}{\pi w_0^2}\exp\left(-\frac{2r^2}{w_0^2}\right), \end{aligned} \tag{A2}$$

where $r = \sqrt{x^2+y^2}$ and P_0 represent the radius of the beam in cross section and the laser power, respectively. Therefore, the intensity in the medium can be expressed as

$$I(r,z) = \frac{2P_0}{\pi w_0^2}\exp\left(-\frac{2r^2}{w_0^2} - \alpha z\right). \tag{A3}$$

The power absorbed by the volume element $r\mathrm{d}r\mathrm{d}\theta\mathrm{d}z$ of a medium can be computed as

$$A(r,z) = \{I(r,z) - I(r,z+\mathrm{d}z)\} r\mathrm{d}r\mathrm{d}\theta$$
$$= -\frac{\partial I(r,z)}{\partial z} r\mathrm{d}r\mathrm{d}\theta\mathrm{d}z$$
$$= \frac{2P_0}{\pi w_0^2}\alpha \exp\left(-\frac{2r^2}{w_0^2} - \alpha z\right) r\mathrm{d}r\mathrm{d}\theta\mathrm{d}z. \quad \text{(A4)}$$

Thus, the total laser power absorbed by a CML of thickness d_{CML} becomes

$$A_{\mathrm{CML}} = -\int_0^\infty \mathrm{d}r \int_0^{2\pi} \mathrm{d}\theta \int_0^{d_{\mathrm{CML}}} r\frac{\partial I(r,z)}{\partial z}\mathrm{d}z$$
$$= P_0\{1 - \exp(-\alpha d_{\mathrm{CML}})\}. \quad \text{(A5)}$$

[1] B. P. Abbott *et al.*, Observation of Gravitational Waves from a Binary Black Hole Merger, Phys. Rev. Lett. **116**, 061102 (2016).

[2] B. P. Abbott *et al.*, Gravitational waves and gamma-rays from a binary neutron star merger: GW170817 and GRB 170817a, Astrophys. J. **848**, L13 (2017).

[3] Y. Utsumi *et al.*, J-GEM observations of an electromagnetic counterpart to the neutron star merger GW170817, Publ. Astron. Soc. Jpn. **69**, 101 (2017).

[4] J. D. E. Creighton and W. G. Anderson, *Gravitational-Wave Physics and Astronomy: An Introduction to Theory, Experiment and Data Analysis* (Wiley-VCH, New York, 2011).

[5] J. Aasi *et al.*, Advanced LIGO, Classical Quantum Gravity **32**, 115012 (2015).

[6] P. R. Saulson, Thermal noise in mechanical experiments, Phys. Rev. D **42**, 2437 (1990).

[7] M. Punturo *et al.*, The Einstein Telescope: A third-generation gravitational wave observatory, Classical Quantum Gravity **27**, 194002 (2010).

[8] M. Abernathy *et al.*, Einstein Gravitational Wave Telescope Conceptual Design Study: ET-0106C-10, 2011 available at https://tds.virgo-gw.eu/?call_file=ET-0106C-10.pdf.

[9] R. X. Adhikari *et al.*, A cryogenic silicon interferometer for gravitational-wave detection, arXiv:2001.11173.

[10] A. Schroeter, R. Nawrodt, R. Schnabel, S. Reid, I. Martin, S. Rowan, C. Schwarz, T. Koettig, R. Neubert, .M. Thürk, W. Vodel, A. Tünnermann, K. Danzmann, and P. Seidel, On the mechanical quality factors of cryogenic test masses from fused silica and crystalline quartz, arXiv:0709.4359.

[11] R. Nawrodt, A. Zimmer, T. Koettig, C. Schwarz, D. Heinert, M. Hudl, R. Neubert, M. Thürk, S. Nietzsche, W. Vodel, P. Seidel, and A. Tünnermann, High mechanical Q-factor measurements on silicon bulk samples, J. Phys. Conf. Ser. **122**, 012008 (2008).

[12] C. A. Swenson, Recommended values for the thermal expansivity of silicon from 0 to 1000 K, J. Phys. Chem. Ref. Data **12**, 179 (1983).

[13] M. J. Keevers and M. A. Green, Absorption edge of silicon from solar cell spectral response measurements, Appl. Phys. Lett. **66**, 174 (1995).

[14] K. Somiya, Detector configuration of KAGRA: The Japanese cryogenic gravitational-wave detector, Classical Quantum Gravity **29**, 124007 (2012).

[15] Y. Aso, Y. Michimura, K. Somiya, M. Ando, O. Miyakawa, T. Sekiguchi, D. Tatsumi, and H. Yamamoto, Interferometer design of the KAGRA gravitational wave detector, Phys. Rev. D **88**, 043007 (2013).

[16] Y. Enomoto, Fogged ITMY, http://klog.icrr.u-tokyo.ac.jp/osl/?r=9377 (2019).

[17] K. Hasegawa, T. Akutsu, N. Kimura, Y. Saito, T. Suzuki, T. Tomaru, A. Ueda, and S. Miyoki, Molecular adsorbed layer formation on cooled mirrors and its impacts on cryogenic gravitational wave telescopes, Phys. Rev. D **99**, 022003 (2019).

[18] J. Steinlechner and I. W. Martin, Thermal noise from icy mirrors in gravitational wave detectors, Phys. Rev. Research **1**, 013008 (2019).

[19] S. Miyoki, T. Tomaru, H. Ishitsuka, M. Ohashi, K. Kuroda, D. Tatsumi, T. Uchiyama, T. Suzuki, N. Sato, T. Haruyama, A. Yamamoto, and T. Shintomi, Cryogenic contamination speed for cryogenic laser interferometric gravitational wave detector, Cryogenics **41**, 415 (2001).

[20] J. Degallaix, C. Michel, B. Sassolas, A. Allocca, G. Cagnoli, L. Balzarini, V. Dolique, R. Flaminio, D. Forest, M. Granata, B. Lagrange, N. Straniero, J. Teillon, and L. Pinard, Large and extremely low loss: The unique challenges of gravitational wave mirrors, J. Opt. Soc. Am. A **36**, C85 (2019).

[21] S. L. Danilishin, C. Gräf, S. S. Leavey, J. Hennig, E. A. Houston, D. Pascucci, S. Steinlechner, J. Wright, and S. Hild, Quantum noise of non-ideal Sagnac speed meter interferometer with asymmetries, New J. Phys. **17**, 043031 (2015).

[22] L. Pinard, C. Michel, B. Sassolas, L. Balzarini, J. Degallaix, V. Dolique, R. Flaminio, D. Forest, M. Granata, B. Lagrange, N. Straniero, J. Teillon, and G. Cagnoli, Mirrors used in the LIGO interferometers for first detection of gravitational waves, Appl. Opt. **56**, C11 (2017).

[23] K. Hasegawa, Ph.D. thesis, The University of Tokyo, 2020.

[24] J.-Y. Vinet, V. Brisson, and S. Braccini, Scattered light noise in gravitational wave interferometric detectors: Coherent effects, Phys. Rev. D **54**, 1276 (1996).

[25] R. Takahashi, K. Arai, S. Kawamura, and M. R. Smith, Direct measurement of the scattered light effect on the sensitivity in TAMA300, Phys. Rev. D **70**, 062003 (2004).

[26] J. M. Elson, J. P. Rahn, and J. M. Bennett, Relationship of the total integrated scattering from multilayer-coated optics to angle of incidence, polarization, correlation length, and roughness cross-correlation properties, Appl. Opt. **22**, 3207 (1983).

[27] J. E. Harvey, N. Choi, S. Schroeder, and A. Duparr, Total integrated scatter from surfaces with arbitrary roughness, correlation widths, and incident angles, Opt. Eng. **51**, 013402 (2012).

[28] C. A. Mack, Analytic form for the power spectral density in one, two, and three dimensions, J. Micro/Nanolithography MEMS MOEMS **10**, 040501 (2011).

[29] D. T. Limmer and D. Chandler, Theory of amorphous ices, Proc. Natl. Acad. Sci. U.S.A. **111**, 9413 (2014).

[30] V. Kofman, J. He, I. L. ten Kate, and H. Linnartz, The refractive index of amorphous and crystalline water ice in the UV–vis, Astrophys. J. **875**, 131 (2019).

[31] S. G. Warren and R. E. Brandt, Optical constants of ice from the ultraviolet to the microwave: A revised compilation, J. Geophys. Res. Atmos. **113**, D14220 (2008).

[32] B. Schmitt, E. Quirico, F. Trotta, and W. M. Grundy, *Optical Properties of Ices From UV to Infrared* (Springer, Dordrecht, Netherlands, 1998), pp. 199–240.

[33] T. Akutsu *et al.*, First cryogenic test operation of underground km-scale gravitational-wave observatory KAGRA, Classical Quantum Gravity **36**, 165008 (2019).

[34] K. Komori, Y. Michimura, and K. Somiya, Parameters for the latest estimated sensitivity of KAGRA, JGW-T1707038 (2017), https://gwdoc.icrr.u-tokyo.ac.jp/cgi-bin/DocDB/ShowDocument?docid=9537.

[35] R. Lawrence, M. Zucker, P. Fritschel, P. Marfuta, and D. Shoemaker, Adaptive thermal compensation of test masses in advanced LIGO, Classical Quantum Gravity **19**, 1803 (2002).

[36] J. B. Paul, L. Lapson, and J. G. Anderson, Ultrasensitive absorption spectroscopy with a high-finesse optical cavity and off-axis alignment, Appl. Opt. **40**, 4904 (2001).

[37] F. Nehm, S. Schubert, L. Mller-Meskamp, and K. Leo, Observation of feature ripening inversion effect at the percolation threshold for the growth of thin silver films, Thin Solid Films **556**, 381 (2014).